Numerical and remote techniques for operational beach management under storm group forcing

Verónica Morales-Márquez[1], Alejandro Orfila[1], Gonzalo Simarro[2], Lluís Gómez-Pujol[3],
Amaya Álvarez-Ellacuría[1], Daniel Conti[1], Álvaro Galán[4], Andrés F. Osorio[5], and Marta Marcos[1,6]

[1]IMEDEA (UIB-CSIC), Mediterranean Institute of Advanced Studies, St. Miquel Marquès 21, 07190, Esporles, (Illes Balears, Spain)
[2]ICM, Institute of Marine Sciences, Passeig Marítim de la Barceloneta 37-49, 08003 Barcelona, (Catalunya, Spain)
[3] Earh Sciences Research Group, Department of Biology, University of the Balearic Islands, Ctra. Valldemossa km 7.5, 07122 Palma (Illes Balears, Spain)
[4]ETSI Caminos, Canales y Puertos, University of Castilla-La Mancha, Av. Camilo José Cela s/n, 13071 Ciudad Real, (Castilla-La Mancha, Spain)
[5]OCEANICOS Research Group. Universidad Nacional de Colombia Cr. 80, 65-223 (Medellin, Colombia)
[6]Department of Physics, University of the Balearic Islands, Ctra. Valldemossa km 7.5, 07122 Palma (Illes Balears, Spain)

Correspondence: Alejandro Orfila (aorfila@imedea.uib-csic.es)

Abstract. The morphodynamic response of a microtidal beach under a storm group is analyzed, and the effects of each individual event inferred from a numerical model, in situ measurements and video imaging. The first storm, with moderate conditions ($H_s \sim 1\,\mathrm{m}$ during 6 hours), eroded the aerial beach and generated a submerged sandbar in the breaking zone. The bar is further directed offshore during the more energetic second event ($H_s = 3.5\,\mathrm{m}$ and 53 hours). The third storm, similar to the first one, hardly affected the beach morphology, which stresses the importance of the beach configuration previous to a storm. The volume of sand mobilized during the storm group was around 17.65 m^3/m. During the following months, which were characterized by mild wave conditions, the dry beach recovered half of the volume of sand that was transported offshore during the storm group (~ 9.27 m^3/m). The analysis of beach evolution shows two different characteristic time scales for the erosion and the recovery processes associated with storm and mild conditions respectively. Besides, the response depends largely on the previous beach morphological state. The work also stresses the importance of using different tools (video-monitoring, modeling and field campaign) to analyze beach morphodynamics.

1 Introduction

Evolution of sandy coasts at all temporal scales has been a topic of wide interest over the past decades since sandy beaches and dune systems are the first natural lines of coastal defense against flooding and erosion hazards (Callaghan and Roshanka, 2009; Hallegatte et al., 2013), being at the same time attractive environments in terms of leisure activities and tourism economy (e.g., Jiménez et al., 2011; Bosello et al., 2012; Luijendijk et al., 2018). The maintenance of these areas is crucial for the coastal

defense and, at the same time, the coastal tourism seems to be one main target for beach erosion management (Semeoshenkova and Newton, 2015). For instance, in Spain, beaches represent only the 0.01% of the land surface, producing up to 10% of its gross domestic product. Beach management tends to be reactive rather than proactive, solving the problems as they appear and without a long term planning.

5   Mitigation of coastal erosion and preservation of coastal areas represent essential aspects of the Protocol on Integrated Coastal Zone Management in the Mediterranean and is included into the objectives of most countries' national regulations and policies in Europe (Semeoshenkova and Newton, 2015). It is already known that decisions concerning coastal management actions should be based using the best available science, and developing new tools that take into account physical, natural and socio-economic characteristics of beaches (Ariza, 2010; Tintoré et al., 2009). This makes it necessary to transfer the knowledge

10   from scientists to managers in an effective way, which nowadays an challenging matter.

    Regarding the management associated to coastal erosion issues, several purposes have recently arisen to improve the managers decisions or, at least, to provide them quality data of the areas of study (Ferreira et al., 2017). One of the main issues in coastal erosion is the response of coastlines to both individual storms and storm groups since the behaviors are quite different (Loureiro et al., 2012; Vousdoukas et al., 2012; Houser, 2013; Coco et al., 2014; Masselink and van Heteren, 2014; Senechal

15 et al., 2015; Masselink et al., 2016, i.e.). Single storms can result in significant beach erosion within a few hours, whereas a sequence of storms can have a large and complex impact on beach morphology whose final effects remain difficult to quantify and to predict (Ferreira, 2005; Frazer et al., 2009).

    Storm waves and their associated water-level conditions are key drivers in the shoreline dynamics. Shoreline response to successive storms can be dependent on storm energy thresholds as well as on the feedback mechanisms associated with the

20 beach morphology and the presence or absence of former impacts (Ciavola and Stive, 2012). There are many examples that have shown that shorelines can recover relatively well from erosion triggered by storms and that this recovery can be quick, from few days or weeks (Birkemeier, 1979; Vousdoukas et al., 2012) to a couple of months (Wang et al., 2006). Therefore, the resilience of beaches, understood as their capacity to recover from a major storm, is related to the combination of sediment reservoirs, arrangement of three-dimensional beach morphology (i.e., sand bar type and location, beach slope, etc.) and to the

25 beach memory (Jara et al., 2015).

    Recent works, as the one by Vousdoukas et al. (2012), have shown that the observed morphological change during consecutive storms has a strong dependence on the initial beach morphology. These authors, departing from field experiments in southern Portugal, stated that beach recovery did not maintain the pace with storms frequency and that storms can have a dramatic impact on the erosion if they occur grouped. In addition, other works dealing with storm impact in shoreline dynamics in

30 the Bay of Biscay (SE France) have suggested that energetic events are probably not the only drivers of erosion processes, since significant beach erosion has been characterized under very calm conditions following energetic events (Senechal et al., 2015). In a similar way, observations from a detailed field campaign involving daily beach surveys at Truc Vert beach (Bordeaux, France) during a sequence of storms demonstrated that a sequence of extreme storms does not necessarily result in cumulative erosion, possibly because of the interplay between water levels, the angle of wave approach and the pre-existing beachface

35 conditions (Coco et al., 2014).

The goal of this contribution is first to study the effect of a storm group on the morphology of a beach system and secondly to present a multiplatform approach to help beach managers to make an insight-driven decisions concerning beach erosion management through the use of the data available in the beach and the operational run of numerical models. Here, we present the explanation of temporal patterns of beach accretion and erosion under consecutive storm events at an intermediate microtidal

5 carbonate beach by using the dataset available on the studied beach, high-frequency data on shoreline positions and crosshore profiles extracted from coastal videomonitoring techniques, RTK and echosounding surveys, concurrent hydrodynamic measurements, and the use of numerical models widely validated in order to fill gaps in the dataset.

2 Field description

Cala Millor is a semi-stretched beach $1.7\,\mathrm{km}$ in length and ranging between 15 and $30\,\mathrm{m}$ in beach width. It is located in the

10 Northeastern coast of Mallorca Island (Western Mediterranean Sea, Fig. A1). Sediments are mainly composed of well-sorted medium to coarse biogenic carbonate sand with a grain diameter D_{50} between 0.3 and $0.6\,\mathrm{mm}$ (Gómez-Pujol et al., 2011). The beach area is around $1.4\,\mathrm{km}^2$ with a bottom colonized by the endemic *Posidonia oceanica* meadow at depths from 6 to $35\,\mathrm{m}$ (Infantes et al., 2009). This meadow increases bottom roughness reducing near bed velocity, modifying the sediment transport (Koch et al., 2007; Infantes et al., 2009, 2012) and increasing wave attenuation (Luhar et al., 2013).

15 From a morphodynamic point of view, Cala Millor is an intermediate beach with a highly dynamic configuration of bars and troughs, presenting intense variations in the bathymetry related to sandbar movement (Álvarez-Ellacuría et al., 2011; Gómez-Pujol et al., 2011).

Tides are negligible (the tidal amplitude is less than $0.25\,\mathrm{m}$) although other surge components such as those induced by wind or atmospheric pressure can increase the sea level up to 1 m (Basterretxea et al., 2004). The beach is open to the east and, due

20 to the semi-enclosed configuration, is well exposed to waves from the NNE to the SE (Enríquez et al., 2017). Significant wave height (H_s) at deep waters is usually bellow $0.9\,\mathrm{m}$ although frequent storms accounting 2% of time increase H_s up to 5 m, with a return period of 1.5 years (Tintoré et al., 2009).

Cala Millor is one of the most important tourist resorts created in the eastern coast of Mallorca –more than $60,000$ visitors during the summer period– and with a long history of sand nourishment and coastal management approaches (Tintoré et al.,

25 2009).

Since November 2010 the Balearic Islands Coastal Observing and Forecasting System (SOCIB) is monitoring Cala Millor by means of coastal video monitoring, moored instruments and a periodic program of beach profile and sediment characterization (Tintoré et al., 2013). Along Cala Millor beach, over short temporal scales, shoreline position changes are not always homogeneous (Fig. A2, a) and it is possible to appreciate some different behaviors and responses to the wave climate. Cala

30 Millor has experienced at least 19 events with significant wave height at 25 meters depth over 2 m between November 2010 and January 2017 (Fig. A2, b). Some of these events are isolated storms (e.g., April 2013) while others act in groups (e.g., January 2015). Fig. A2,a shows the alongshore anomaly of shoreline distances for the period between November 2010 to January 2017. The correlation between beach face response and sea conditions is not clear: there are storms that, even though Cala Millor

is not a pocket beach, are giving rise to apparent temporary rotation, whereas others appear as a general shoreline advance or retreat. Nevertheless, from the averaged alongshore shoreline width anomaly (Fig. A2, c) it can be inferred a clear change in beach behavior since April 2014, just after a group of storm events that will be analyzed below. Despite the beach eventually recovers the former alongshore width, it is observed a net shoreline recession.

5   In March 2014, just few days before the above mentioned storm group event, a field experiment was carried out in Cala Millor in order to characterize the beach morphology. This experiment produced detailed bathymetries and beach profiles were measured before the storms and also wave recorders were installed at different depths, as detailed below. Later, in June 2014, it was carried out another detailed beach survey and bathymetry belonging to the SOCIB's periodic beach monitoring program (Tintoré et al., 2013). Unfortunately, even though the April 2014 storm group seems to be critical for the beach width evolution,

10   there are no bathymetric data available immediately after the storms. Nevertheless, the amount of available data before and after the storm group impacts makes this an opportunity to validate and generate numerical proxies that contribute to unravel the beach response to the storm group.

3 Data and methods

This paper partially deals with datasets produced during the Riskbeach experiment, performed by the SOCIB, the Mediter-

15   ranean Institute for Advanced Studies (IMEDEA) and the Institute of Marine Sciences (ICM-CSIC) in Cala Millor from March 17th to March 26th 2014. This experiment was designed to study the response and recovery of an intermediate beach to usual (one year return period) storm conditions and the related sediment transport processes and morphological changes. During the experiment some instruments, detailed in Fig. A1, were installed in a central section of the beach to obtain high resolution sediment and hydrodynamical data. In this paper we will employ the wave and currents recorder data (AWAC) moored at 25

20   m depth. Measurements were completed with bathymetric surveys, sediment samples and videomonitoring products. After the experiment (just from March 26th) large waves resulted in a significant morphological change of the beach, once the field survey was finished and the echosounding equipment was dismantled. To assess the effects of these storms we combine numerical modelling with videomonitoring techniques to infer the beach profiles that will help us to understand the changes in the beach morphology before and after the storm group.

25   Fig. A1 and Fig. A3 summarize the approach developed in this study showing what type of data comes from different instrumental approaches (i.e., direct measurements from bathymetric and DGPS-RTK surveys) and which ones are inferred from numerical modelling and video images (indirect measurements). According to that, results will be organized in two sections: first, profiles obtained by direct methods and, second, the results related to the use of these data sources for unraveling the beach erosion and recovery time scales.

3.1 Wave conditions

Offshore wave conditions (significant wave height, H_s, peak period T_p and wave direction at 50 m depth every three hours) are obtained from a reanalysis of a 60 years wave model output produced by the Spanish Harbor Authority (http://www.puertos.es/es-

es/oceanografia/Paginas/portus.aspx). The mean H_s for the period of study is $0.9\,\mathrm{m}$ with a mean peak period (T_p) of 6 s. During the experiment (March 17$^{\mathrm{th}}$ to March 26$^{\mathrm{th}}$ 2014), wave conditions were measured with an AWAC-system moored at intermediate waters ($25\,\mathrm{m}$ depth) in the central part of the beach.

Offshore wave conditions show three storms during the period of study (Fig. A4). We define here storm as sustained wave
5   conditions during at least 6 hours with $H_s > 1\,\mathrm{m}$. Gómez-Pujol et al. (2011) suggested this threshold as the conditions required to generate a significant impact along beach morphology and sediment properties. The experiment started on March 17$^{\mathrm{th}}$ after a period of moderate conditions with H_s close to 1 m that did not result in significant morphological changes. The first storm, S1 (see Fig. A4,a), occurred on March 26$^{\mathrm{th}}$, just after the instruments were moved away, with a maximum significant wave height $H_s = 1.5\,\mathrm{m}$ and $T_p = 9.9\,\mathrm{s}$ from the SE (Fig. A4,c) and a duration of 7 hours. The second storm, S2, beginning on
10 March 28$^{\mathrm{th}}$, lasted 53 hours and peaked during the evening of March 29$^{\mathrm{th}}$ with a maximum H_s of 3.4 m and T_p of 10.4 s. The estimated return period for S2 storm is around 1.2 years. Nevertheless, the return period just refers to the significant wave height threshold, despite the storm duration and persistence of wave height was 38 hours with $H_s > 2\,\mathrm{m}$ which is unusual. Wave conditions started to build up again on April 2$^{\mathrm{nd}}$ 2014 after a short period of relatively small waves ($H_s < 1\,\mathrm{m}$). The third storm, S3, April 2$^{\mathrm{nd}}$ to 3$^{\mathrm{rd}}$, peaked 4 days after the former storm with maximum H_s of 1.3 m and T_p of 7.8 s (Fig. A4,a
15 and Fig. A4,b) during 48 hours. The following two months were characterized by mild conditions wich will be used to study the beach recovery after the storm groups.

3.2 Beach morphology

The topographic surveys were performed from March 17$^{\mathrm{th}}$ to March 26$^{\mathrm{th}}$ using a DGPS-RTK with submetrical resolution for both the aerial and the submerged beach (up to 1 m depth). Additionally, for submerged beach, bathymetric data was
20 obtained using a Biosonics DE-4000 echosounder with a DGPS which allowed dense mapping from 0.5 to 10.0 m in depth. On March 17$^{\mathrm{th}}$, an initial full bathymetry was acquired and between March 18$^{\mathrm{th}}$ and March 26$^{\mathrm{th}}$, 9 daily cross-shore profiles were measured along the beach (see Fig. A1 for the location of the profiles). An additional full bathymetry was performed on June 12$^{\mathrm{th}}$ for control purposes. Elevations were referenced to the Balearic Islands Ordinance Survey mean sea level and the horizontal position referenced to UTM coordinates systems (Gómez-Pujol et al., 2011). These data covers the area between the
25 boulevard sea wall and the lower shoreface (ca. 8 m in depth).

3.3 Sediment characteristics

Sediment samples were collected from aerial beach (+2 m) to 6 m depth at one of the central cross-shore transects (profile #07, Fig. A1). Sediments in the dry beach and up to 1 m depth were collected by dragging on the bottom a plastic bag inserted in an oval metallic frame being their vertical penetration about 2-4 cm and for greater depths, throwing a clamshell bucket from
30 a boat. The weight of samples ranged from 200 to 500 g. After collection, samples were soaked in fresh water for 4 hours and drained before being trapped for 24 hours. Sediment were analyzed using a laser granulometer and grain size obtained through the method described by Folk and Ward (1957) using Gradistat software (Blott and Pye, 2001).

3.4 Video monitoring

Coastal monitoring using video images is a practical and widely used technique since the advent of Argus (Holland et al., 1997). Since then, several systems (Cam-era, Horus, Cosmos, Beachkeeper, Ulises, etc.) mimic the Argus philosophy with the objective of providing continuous measurements of coastal processes in a non-supervised and autonomous procedure. Here,

5   we use one of such approaches, SIRENA/Ulises (Nieto et al., 2010; Simarro et al., 2017), which has been operating since 2009 in Cala Millor. The system is composed of five CCD cameras connected to a server acquiring daily images (Gómez-Pujol et al., 2013). The five cameras encompass an alongshore distance of around 1.7 km, largely including the monitored area. We have used the timestacks, consisting of pseudo-images built with all pixel observation taken at 7.5 Hz at a predefined cross shore transect during the first 10 minutes of each hour, to infer the beach profile with the inversion of the wave dispersion

10 relationship. The underlying idea in the inversion method is that the wave speed for progressive waves can be measured from its visible signature at consecutive snapshots to estimate the bathymetry using linear wave theory at the observed cross-shore transect (Stockdon and Holman, 2000).

Adopting the linear wave theory, the wave celerity c for shallow water waves ($kh < \pi/10$ where k is the wave number and h the local water depth) is

15 $$c^2 = g \cdot h, \tag{1}$$

where g is the gravitational acceleration.

Timestack images (Fig. A5,a) are pre-processed to convert the RGB data to a tractable intensity matrix. First, original timestacks, with spatial and temporal dimensions $(n_x, n_t) = (650, 4500)$, are re-sampled by removing pixels at the dry beach as well as at the outer domain (intermediate waters) where each pixel corresponds to large distances and are thus not useful

20 to measure hydrodynamic processes, obtaining final images with spatial and temporal dimensions of $(\hat{n}_x, n_t) = (460, 4500)$ (Fig. A5b). A quadratic filter with a time window of three seconds is applied to smooth the intensity timewise, and for each cross-shore position the temporal mean subtracted. From the intensity matrix $I(x,t)$, the wave frequency is obtained as the main component of the FFT in the time domain which is constant along the cross-shore dimension. A FFT is performed for each of the 460 cross-shore time series and the wave frequency, f, found as the mode of all resulting peaks.

25 Once f is known, the spatial component of the wave phase function (Fig. A5b), is evaluated following (Stockdon and Holman, 2000) as,

$$\phi = \arctan\left\{\frac{\text{Im}(I(x,\omega))}{\text{Re}(I(x,\omega))}\right\}, \tag{2}$$

and the wave celerity obtained as,

$$c = \frac{2\pi f}{\partial\phi/\partial x}. \tag{3}$$

30 The beach profile is finally obtained from Eq. (1).

3.5 Numerical modelling

Morphological evolution was assessed using the XBeach (eXtreme Beach behavior) model (Roelvink et al., 2009), which resolves the hydrodynamic processes of both the short waves (refraction, shoaling and breaking) and the long waves (generation, propagation and dissipation). The model has been extensively validated with laboratory data as well as with field observations

5 to study the morphological response of beach and sandy dunes, mostly under storm conditions. Here, we will apply the model to analyze the storm group period.

The initial bathymetry (of March 17$^{\text{th}}$) was discretized in an orthogonal rectangular grid evenly spaced with a resolution of $\Delta x = 7.44\,\text{m}$ in the cross-shore direction and with $\Delta y = 15.86\,\text{m}$ in the along-shore direction. Hourly JONSWAP spectra measured with the AWAC, were propagated from the offshore boundary to the coast for the period of March 17$^{\text{th}}$ to April

10 8$^{\text{th}}$, after S3 (summing up 528 runs of one hour of real time). The offshore boundary was imposed as absorbing-generating (weakly-reflective) boundary condition and the lateral boundaries as Neumann-type where the longshore gradients were set to zero. The incoming wave directions in almost all simulations were from the East perpendicular to the shoreline (Fig. A4c).

Sediment characteristic measured before the experiment (D_{50} and D_{90}) were interpolated to the model grid points, according to their depth. The dimensionless porosity of the sediment was set to $30\,\%$ and the density considered as $2650\,\text{kg/m}^3$.

15 4 Results and Discussion

4.1 Bathymetry extraction from model and video images

The analyses based on XBeach and on timestacks are used to obtain the bathymetry and beach profiles to address changes in sediment mass balance. The initial condition for the seabed was the bathymetry measured before the storms (March 17$^{\text{th}}$) and the numerical model was run for the period between March 17$^{\text{th}}$ to April 8$^{\text{th}}$, as mentioned. For each day, 9 different profiles

20 were extracted from the resulting modeled seabed at the same locations of the measured cross-shore profiles and the process was repeated for the whole period of the experiment. Table 1 shows the mean and maximum differences in height between the measured profiles and the XBeach modeled profiles from March 17$^{\text{th}}$ to March 26$^{\text{th}}$ as well as the profile where the maximum difference is obtained. The profiles derived from the model compare well with the measured ones from the emerged beach ($h = 2\,\text{m}$) to the depth of closure ($h = -7\,\text{m}$). Mean differences range between 0.13 to $0.16\,\text{m}$ whereas maximum differences

25 attend ca. $1\,\text{m}$. Therefore the modeled bathymetries (XBeach) can be considered as an efficient and reliable tool for unravelling the beach storm effects.

As an additional source of data, a cross-shore seabed profile in the SIRENA/Ulises central camera (Fig. A6) was obtained following the above described methodology. Table 2 compares the cross-shore profiles derived from timestacks against the instrumental measured profiles for the period between March 19$^{\text{th}}$ to April 26$^{\text{th}}$ (there were not timestacks available for

30 March 17$^{\text{th}}$ and 18$^{\text{th}}$). Since the timestack was defined in a cross-shore transect located between profiles #07 and #09, in situ measurements were daily interpolated to the timestack transect for comparison purposes. Mean differences between profiles from in situ measurements and from video images range between 0.10 and $0.40\,\text{m}$ (Table 2), whereas the maximum difference

range between 0.40 and $1.56\,\mathrm{m}$. The largests differences tend to be located at deep profile positions where the model is known to perform worse since the accepted assumption on Eq. (1) only is valid for shallow waters. In general, there is a good agreement between both sets of data.

Both comparisons, XBeach vs. instrumental and timetack vs. instrumental, resulted in mean error values and maximum error values of the same order of magnitude, respectively 0.10 to $0.40\,\mathrm{m}$ and ca. $1\,\mathrm{m}$. This allows us to compare beach sediment mass-balance before and after the storm group as well as during the longer period of calm after the storms using different datasets and different techniques. This allows a correct management of the beach avoiding unnecessary engineering works between touristic seasons.

4.2 Beach morphological response to storms and recovery

Although the individual storms were not exceptional in terms of intensity, their occurrence as a storm group had a significant imprint on the beach morphology. The initial bathymetry, performed before the storm group (on March 17th 2014), showed a sinuous-parallel and patchily bar at $-1\,\mathrm{m}$ and a cross-shore profile with attenuated secondary forms with a mean slope of 2.6%, whereas the bathymetry obtained for April 8th 2014 from XBeach shows a marked dissipative configuration (see Fig. A7). The seabed variation after the storm group (S1, S2 and S3, in Fig. A4,a) is presented in Fig. A8,a. This morphological change is obtained as the difference between the bathymetry obtained with XBeach after storm S3 (April 8th) and the initial bathymetry. The effect of consecutive storms is to erode mainly the dry beach mobilizing the sediment from the berm to depths between -1 m and -5 m forming a bar (around 100 meters from the shoreline, Fig. A8,a). The sediment mobilized to the bar is around $2.69 \cdot 10^4$ m^3 and is provided by the dry beach, where the volume loss is estimated as $3.01 \cdot 10^4$ m^3. The redistribution can be also examined by analysing the profile at the center of the beach using video images. Fig. A9,a shows the beach profile change using video images from March 19th (the selection of the 19th was made since no images were available for the previous days) to April 8th (after S3).

Deepening in the beach response to the storm group, we have analyzed the differences between the initial bathymetry (March 17th 2014, previous to S1) and the bathymetries after storms S1, S2 and S3 (March 28th, April 1st and 8th respectively) obtained from XBeach. Fig. A10 shows the differences, i.e., the impact of each of the storms. The first storm, S1, with moderate H_s and short duration, produces erosion at the beach face (volume loss of $1.18 \cdot 10^4$ m^3) accumulating large volumes of sand between -1 m and -2 m (not shown in Fig. A10). During the second storm, S2, which was the most energetic the beach-face suffered a new episode of intense erosion, with depth variations between 1 m and 1.5 m and moving the bar offshore (Fig. A10,b). The gain in volume in the bar zone was around $1.51 \cdot 10^4$ m^3. Finally, the third storm (S3), with moderate wave heights but with large duration, continued eroding the dry beach with little changes in the submerged beach (Fig. A10,c). This indicates that a sequence of storms does not necessarily result in cumulative erosion, supporting previous findings by Birkemeier et al. (1999) and Coco et al. (2014). The eroded sediment that has been transported offshore but not lost has the capacity to modify the cross-shore morphology and promotes the wave attenuation contributing to the sediment transport feedback.

The three-dimensional beach response to three successive storms highlights the importance of the storm duration in the sedimentary budget. This has been recently addressed in different studies (Ruiz de Alegria-Arzaburu and Masselink, 2010;

Vousdoukas et al., 2012; Coco et al., 2014; Senechal et al., 2015, among others) and particularly for the Mediterran ean by Jiménez et al. (2008). This scenario fits with the usual 'storm-post storm' behavior model (Stive et al., 2002; Archetti et al., 2016) and highlights the need of more research, specially in the physical description and numerical modeling, in order to improve our knowledge of the characterization of the temporal scales associated with the beach sedimentary budget. Here, we

5   found evidences that recovery times, jointly with antecedent morphology, play a crucial role in shoreline and beach dynamics as stated by Senechal et al. (2015) or Jara et al. (2015).

After S3 storm the beach was under relatively calm conditions. A new bathymetry was done on June 12th 2014 allowing us to address the behavior of the beach during this period. Fig. A8,b shows the differences between the the bathymetry at June 12th and the post-storm bathymetry obtained with numerical modeling for April 8th 2014. As seen, two months after the storm

10   group, there was an opposite scenario. The sand reservoir below fed up the shore-face again, but also redistributed sediment along the beach at different depths. The sand volume recovered at the dry beach during this period was $1.58 \cdot 10^{4}$ m^{3} that is half of the volume lost during the storm period. This behavior is confirmed from the analysis of the beach cross-shore profile obtained from the timestack video image. Fig. A9,b shows the difference between the the summer profile (June 12th 2014) and the beach profile after S3 (April 8th 2014) supporting a recovery of the upper part of the beach.

15 **5 Conclusions**

The response of a low energy microtidal beach in front of storm groups on time scales related to processes of beach erosion and accretion has been studied. For this purpose, different techniques and approaches including DGPS-RTK and bathymetry surveys, modeling and video monitoring have been combined. The observations confirm that the previous morphological conditions are crucial for controlling the sediment exchange and the morphological response of the beach.

20   Focusing on the effect of individual storms, the first one mobilizes sand mostly from the dry area generating a parallel bar at depths ~ 1 m modifying the beach profile from near reflective to more dissipative. The effect of S2, lasting for more than 30 hours, is to mobilize a large volume of sediment redistributing the profile along all the beach and generating a large submerged sandbar at depths ~ -2.5 m (~ 100 m from the shoreline). This profile shows to be very efficient in protecting the beach from the third storm, which has a duration of 48 hours, being the sediment mobilized during this event, almost negligible. The largest

25   changes in sediment mobilization occur in the transition from the reflective to the dissipative states, when the beach adjusts its profile to the incoming wave conditions. The combined effects of this storm group confirm that in low energy systems as the one here analyzed, it is necessary to know the previous morphological state in order to properly assess the new beach conditions.

Results highlight the well known different temporal scales for the erosion and accretion in low energetic systems. While

30 offshore sand migration is produced at storm timescales, the onshore sediment transport has a much slower characteristic timescale. In particular, a group of relatively energetic storms has the capacity to generate significant erosion in three days. Despite the moderate conditions and the lack of storms during the next two months only half of the sediment has been recovered. In this study the recovery of the beach has not been documented, neither in sediment mass balance nor in shoreline width.

Nevertheless from Fig. A2,a it can be appreciated that the dry beach remained relatively stable and slightly increased the beach width at the end of 2014. Then in December 2014 and early January 2015, a new set of storm groups events affected the beach and since then the beach shoreline width has not recovered former conditions, despite punctually there has been some advance in shoreline position.

5   Time recovery after storms is a key issue for local beach managers who are pressed by touristic stakeholders to nourish the beach after energetic process in order to reach the quality standards required by beach users. The combined use of remote sensing data, in situ observations and numerical models, should already be integrated in management tools to take short term decisions, as beach nourishment, based on reliable physical data.

Data availability. All data are accessible from http://www.socib.es.

Author contributions. A.O. conceived the idea of the study with the support of V.M., L.G.P., G.S. and M.M.; A.O., G.S. and V.M. developed the methodology with the support of A.A. and D.C.; V.M. produced the results with the support of A.O. and D.C.; A.A. and G.S. and L.G.P. analyzed the results with the support of A.O and V.M. All authors contributed to write the MS.

Competing interests. AO is a member of the editorial board of Ocean Dynamics and Frontiers in Marine Sciences. MM is a member of the editorial board of Frontiers in Marine Sciences

Acknowledgements. Authors acknowledge financial support from MINECO/FEDER through projects MORFINTRA/MUSA (CTM2015-66225-C2-2-P) and CLIMPACT (CGL2014-54246-C2-1-R). V. Morales-Márquez is supported by an FPI grant from the Ministerio de Economía, Industria y Competitividad of the Spanish Government associated to MORFINTRA/MUSA. D. Conti is supported by a PhD fellowship (FPI/1543/2013) granted by the Conselleria d'Educació, Cultura i Universitats from the Government of the Balearic Islands co-financed by the European Social Fund.

References

Álvarez-Ellacuría, A., Orfila, A., Gómez-Pujol, L., Simarro, G., and Obregon, N. : Decoupling spatial and temporal patterns in short-term beach shoreline response to wave climate. *Geomorphology*, 128(3):199–208, 2011.

Anderson, T. R., Frazer, L. N., and Fletcher, C. H.: Transient and persistent shoreline change from a storm. *Geophysical Research Letters*, 37(8). L08401, 2010.

Archetti, R., Paci, A., Carniel, S., and Bonaldo, D. (2016). Optimal index related to the shoreline dynamics during a storm: the case of Jesolo beach. *Natural Hazards and Earth System Sciences*, 16(5):1107–1122, 2016.

Ariza, E.: An analysis of beach management framework in Spain. Study case: the Catalonian coast. *Journal of Coastal Conservation*, 15(4):445–455, 2010.

Basterretxea, G., Orfila, A., Jordi, A., Casas, B., Lynett, P., Liu, P., Duarte, C. M., and Tintoré, J.: Seasonal dynamics of a microtidal pocket beach with *Posidonia oceanica* seabeds (Mallorca, Spain). *Journal of Coastal Research*, 20:1155–1164, 2004.

Birkemeier, W. A.: *The effects of the 19 December 1977 coastal storm on beaches in North Carolina and New Jersey*, volume 47. Coastal Engineering Research Center, 1979.

Birkemeier, W. A., Nicholls, R. J., and Lee, G.-H.: Storms, storm groups and nearshore morphologic change. In *Coastal Sediments*, pages 1109–1122. ASCE, 1999.

Blott, S. J. and Pye, K.: Gradistat: a grain size distribution and statistics package for the analysis of unconsolidated sediments. *Earth surface processes and Landforms*, 26(11):1237–1248, 2001.

Bosello, F., Nicholls, R. J., Richards, J., Roson, R., and Tol, R. S.: Economic impacts of climate change in Europe: sea-level rise, 2012. *Climatic Change*, 112(1):63–81.

Callaghan, D. P. and Roshanka, R.: Quantifying the storm erosion hazard for coastal planning. *Coastal Engineering*, 56(1):90–93, 2009.

Ciavola, P. and Stive, M.: Thresholds for storm impacts along European coastlines: introduction. *Geomorphology*, 143:1–2, 2012.

Coco, G., Senechal, N., Rejas, A., Bryan, K., Capo, S., Parisot, J., Brown, J., and MacMahan, J.: Beach response to a sequence of extreme storms. *Geomorphology*, 204:493–501, 2014.

Enríquez, A.R., Marcos, M., Álvarez-Ellacuría, A., Orfila, A., and Gomis, D.: Changes in beach shoreline due to sea level rise and waves under climate change scenarios: application to the Balearic Islands (western Mediterranean). *Natural Hazards and Earth System Sciences*, 17(7):1075, 2017.

Ferreira, Ó.: Storm groups versus extreme single storms: predicted erosion and management consequences. *Journal of Coastal Research*, 42:221–227, 2005.

Ferreira, O., Viavattene, C., Jimenez, J.A., Bolle, A., das Neves, L., Plomaritis, T.A., McCall, R., van Dongeren, AR.: Storm-induced risk assessment: Evaluation of two tools at the regional and hotspot scale. *Coastal Engineering*, 134:241–253, 2017.

Folk, R. L. and Ward, W. C.: Brazos river bar: a study in the significance of grain size parameters. *Journal of Sedimentary Research*, 27(1):3–26, 1957.

Frazer, L. N., Anderson, T. R., and Fletcher, C. H.: Modeling storms improves estimates of long-term shoreline change. *Geophysical Research Letters*, 36(20), 2009.

Gómez-Pujol, L., Orfila, A., Álvarez-Ellacuría, A., Terrados, J., and Tintoré, J.: *Posidonia oceanica* beach-cast litter in mediterranean beaches: a coastal videomonitoring study. *Journal of Coastal Research*, 2(65):1768–1773, 2013.

Gómez-Pujol, L., Orfila, A., Alvarez-Ellacuría, A., and Tintoré, J.: Controls on sediment dynamics and medium-term morphological change in a barred microtidal beach (Cala Millor, Mallorca, Western Mediterranean). *Geomorphology*, 132(3–4):87 – 98, 2011.

Hallegatte, S., Green, C., Nicholls, R. J., and Corfee-Morlot, J.: Future flood losses in major coastal cities. *Nature Climate Change*, 3(9):802–806, 2013.

5 Holland, K. T., Holman, R. A., Lippmann, T. C., Stanley, J., and Plant, N.: Practical use of video imagery in nearshore oceanographic field studies. *IEEE Journal of oceanic engineering*, 22(1):81–92, 1997.

Houser, C.: Alongshore variation in the morphology of coastal dunes: Implications for storm response. *Geomorphology*, 199:48–61, 2013.

Infantes, E., Terrados, J., Orfila, A., Cañellas, B., and Álvarez-Ellacuria, A.: Wave energy and the upper depth limit distribution of *Posidonia oceanica*. *Botanica Marina*, 52(5):419–427, 2009.

10 Infantes, E., Orfila, A., Simarro, G., Terrados, J., Luhar, M., Nepf, H., et al.: Effect of a seagrass (*Posidonia oceanica*) meadow on wave propagation. *Marine Ecology Progress Series*, 456:63–72, 2012.

Jara, M., González, M., and Medina, R.: Beach memory related to cross-shore processes. *Coastal Sediments 2015: The Proceedings of the Coastal Sediments, 2015*.

Jiménez, J. A., Gracia, V., Valdemoro, H. I., Mendoza, E. T., and Sánchez-Arcilla, A.: Managing erosion-induced problems in nw mediter-
15 ranean urban beaches. *Ocean & Coastal Management*, 54(12):907–918, 2011.

Jiménez, J. A., Guillén, J., and Falqués, A.: Comment on the article "Morphodynamic classification of sandy beaches in low energetic marine environment" by Gómez-Pujol, L., Orfila, A., Cañellas, B., Alvarez-Ellacuria, A., Méndez, FJ, Medina, R. and Tintoré, J. Marine Geology, 242, pp. 235–246, 2007. *Marine Geology*, 255(1):96–101, 2008.

Koch, E. W., Ackerman, J. D., Verduin, J., and van Keulen, M.: Fluid dynamics in seagrass ecology–from molecules to ecosystems. In
20 *Seagrasses: biology, ecologyand conservation*, pages 193–225. Springer, 2007.

Loureiro, C., Ferreira, Ó., and Cooper, J. A. G.: Extreme erosion on high-energy embayed beaches: influence of megarips and storm grouping. *Geomorphology*, 139:155–171, 2012.

Luhar, M., Infantes, E., Orfila, A., Terrados, J., and Nepf, H. M.: Field observations of wave-induced streaming through a submerged seagrass (*Posidonia oceanica*) meadow. *Journal of Geophysical Research: Oceans*, 118(4):1955–1968, 2013.

25 Luijendijk, A., Hagenaars, G., Ranasinghe, R., Baart, F., Donchyts, G. and Aarninkhof, S.: The State of the World's Beaches. *Scientific reports*, 8, 2018.

Masselink, G., Scott, T., Poate, T., Russell, P., Davidson, M., and Conley, D.: The extreme 2013/2014 winter storms: hydrodynamic forcing and coastal response along the southwest coast of england. *Earth Surface Processes and Landforms*, 41(3):378–391, 2016.

Masselink, G. and van Heteren, S.: Response of wave-dominated and mixed-energy barriers to storms. *Marine Geology*, 352:321–347, 2014.

30 Nieto, M. A., Garau, B., Balle, S., Simarro, G., Zarruk, G. A., Ortiz, A., Tintoré, J., Álvarez-Ellacuría, A., Gómez-Pujol, L., and Orfila, A.: An open source, low cost video-based coastal monitoring system. *Earth Surface Processes and Landforms*, 35(14):1712–1719, 2010.

Roelvink, D., Reniers, A., van Dongeren, A., van Thiel de Vries, J., McCall, R., and Lescinski, J.: Modelling storm impacts on beaches, dunes and barrier islands. *Coastal Engineering*, 56(11–12):1133 – 1152, 2009.

Ruiz de Alegria-Arzaburu, A. and Masselink, G.: Storm response and beach rotation on a gravel beach, Slapton Sands, UK. *Marine Geology*,
35 278(1):77–99, 2010.

Senechal, N., Coco, G., Castelle, B., and Marieu, V.: Storm impact on the seasonal shoreline dynamics of a meso-to macrotidal open sandy beach (Biscarrosse, France). *Geomorphology*, 228:448–461, 2015.

Semeoshenkova, V. and Newton, A.: Overview of erosion and beach quality issues in three Southern European countries: Portugal, Spain and Italy. *Ocean & Coastal Management* 118:12–21, 2015.

Simarro, G., Ribas, F., Alvarez, A., Guillen, J., Chic, O., and Orfila, A.: Ulises: An open source code for extrinsic calibrations and planview generations in coastal video monitoring systems. *Journal of Coastal Research*, 33(5):1217–1227, 2017.

Stive, M. J., Aarninkhof, S. G., Hamm, L., Hanson, H., Larson, M., Wijnberg, K. M., Nicholls, R. J., and Capobianco, M.: Variability of shore and shoreline evolution. *Coastal Engineering*, 47(2):211–235, 2002.

Stockdon, H. F. and Holman, R. A.: Estimation of wave phase speed and nearshore bathymetry from video imagery. *Journal of Geophysical Research: Oceans*, 105(C9):22015–22033, 2000.

Tintoré, J., Medina, R., Gómez-Pujol, L., Orfila, A., and Vizoso, G.: Integrated and interdisciplinary scientific approach to coastal management. *Ocean & Coastal Management*, 52(10):493–505, 2009.

Tintoré, J., Vizoso, G., Casas, B., Heslop, E., Pascual, A., Orfila, A., Ruiz, S., Martínez-Ledesma, M., Torner, M., Cusí, S., et al.: Socib: The balearic islands coastal ocean observing and forecasting system responding to science, technology and society needs. *Marine Technology Society Journal*, 47(1):101–117, 2013.

Vousdoukas, M. I., Almeida, L. P. M., and Ferreira, Ó.: Beach erosion and recovery during consecutive storms at a steep-sloping, meso-tidal beach. *Earth Surface Processes and Landforms*, 37(6):583–593, 2012.

Wang, P., Kirby, J. H., Haber, J. D., Horwitz, M. H., Knorr, P. O., and Krock, J. R.: Morphological and sedimentological impacts of Hurricane Ivan and immediate poststorm beach recovery along the Northwestern Florida barrier-island coasts. *Journal of Coastal Research*, 22(6):1382–1402, 2006.

Table 1. Differences between the measured beach profile and the estimation from XBeach. The table shows for each day, the mean difference (in m), the maximum difference (in m) and the profile where is found.

Date	Mean difference	Max difference	
03-2014	(m)	(m)	Profile #
17	0.14	0.77	13
18	0.15	0.54	11
19	0.16	0.89	07
20	0.15	0.65	11
21	0.18	1.05	03
22	0.13	0.62	05
23	0.16	0.77	09
24	0.14	0.73	13
25	0.15	0.65	07
26	0.15	0.61	13

Table 2. Differences in the bathymetry estimation from timestacks. The table shows for each day, the mean difference (in m) and the maximum difference (in m).

Date	Mean difference	Max difference
03-2014	(m)	(m)
19	0.25	0.65
20	0.10	0.40
21	0.23	0.55
22	0.29	0.63
23	0.26	0.69
24	0.39	1.56
25	0.16	0.89
26	0.42	0.88
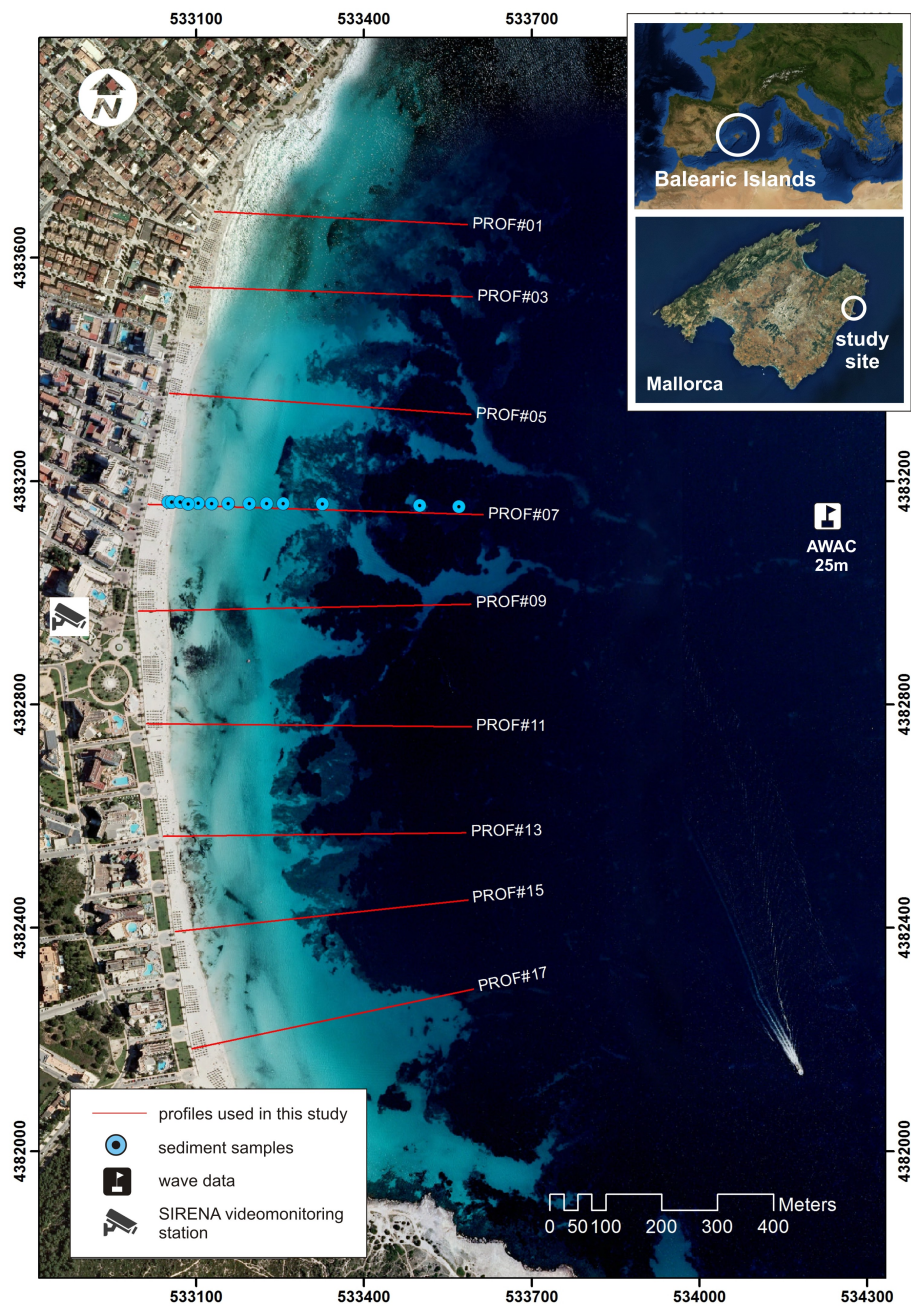
Figure 1. Location of Cala Millor. Red lines indicate the position of the cross-shore beach profiles. Blue dots are the position of the sediment samples. The location of the AWAC and the Sirena remote video station are also indicated.
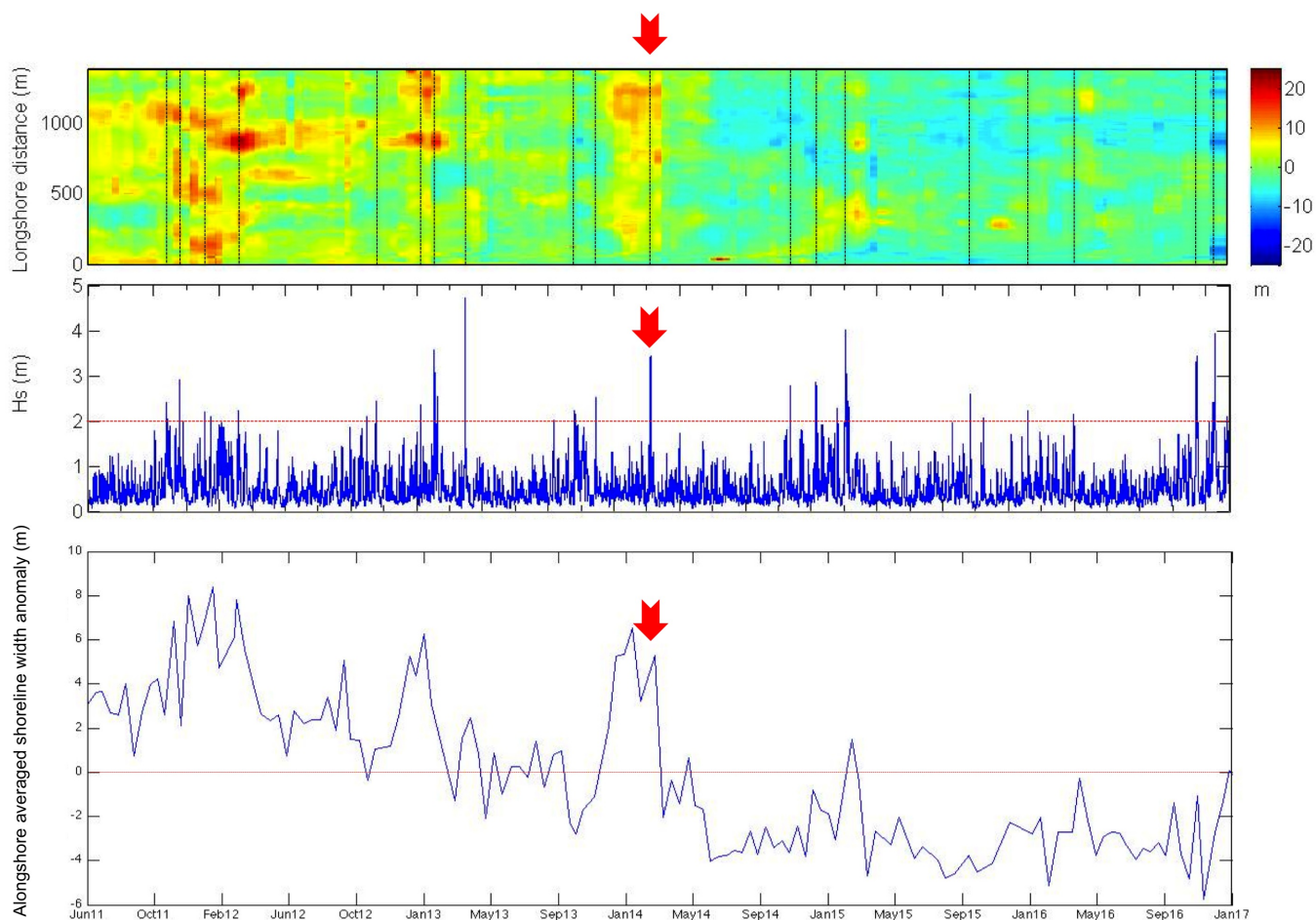
Figure 2. A) Alongshore shoreline width anomaly at Cala Millor from November 2010 to January 2017. Red colors indicate shoreline advance, whereas blue ones indicate shoreline recession. The dashed black lines show the sea storm events larger than 2 m. B) Wave significant height from a wave recorder located at -17 m in the middle of Cala Millor embayment. C) Alongshore averaged shoreline width anomaly at Cala Millor. The red arrows highlight the storm group event at April 2014.
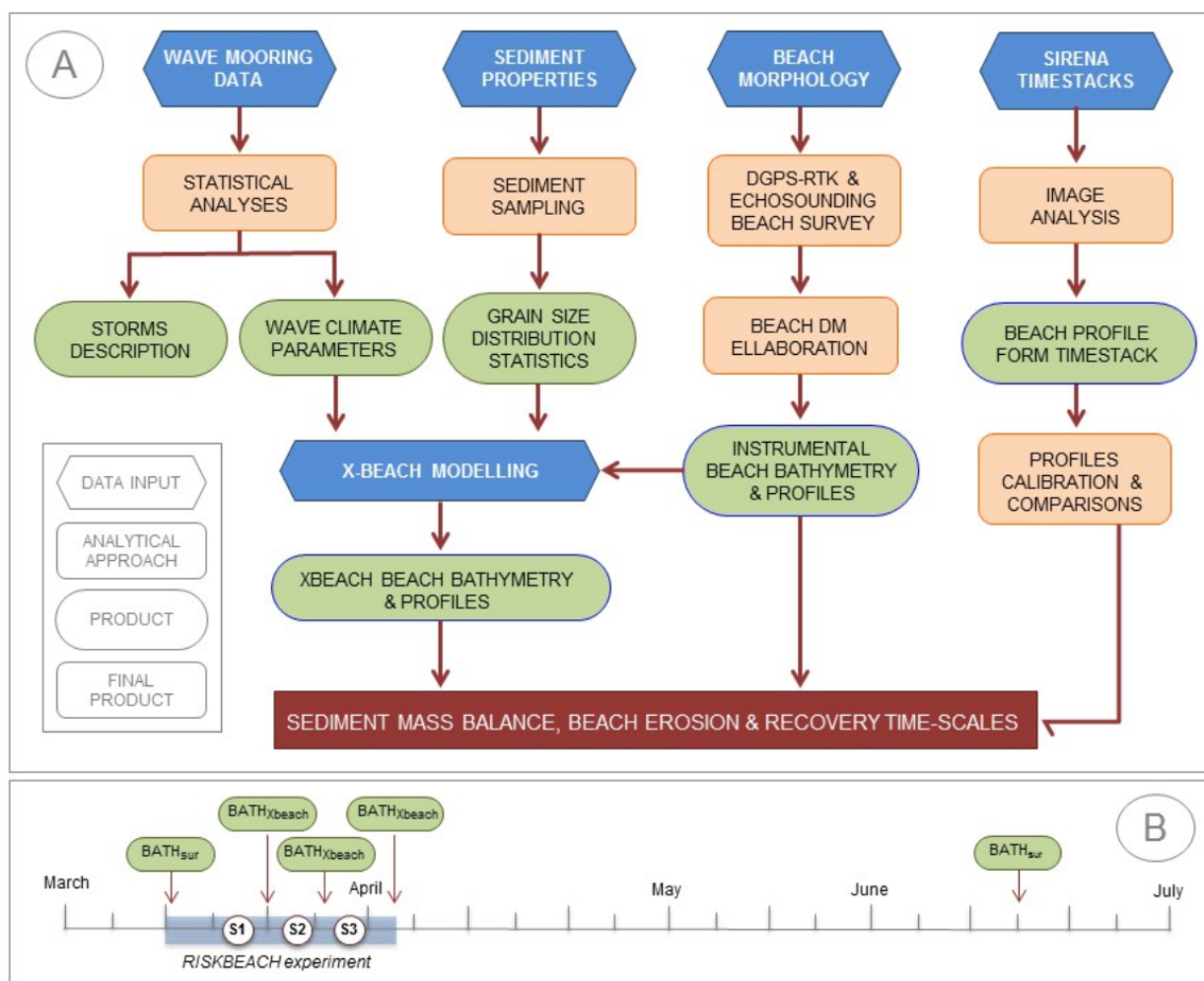
Figure 3. a) Workflow of the aproach followed in the study. b) Calendar showing the date for the samples used in the study.
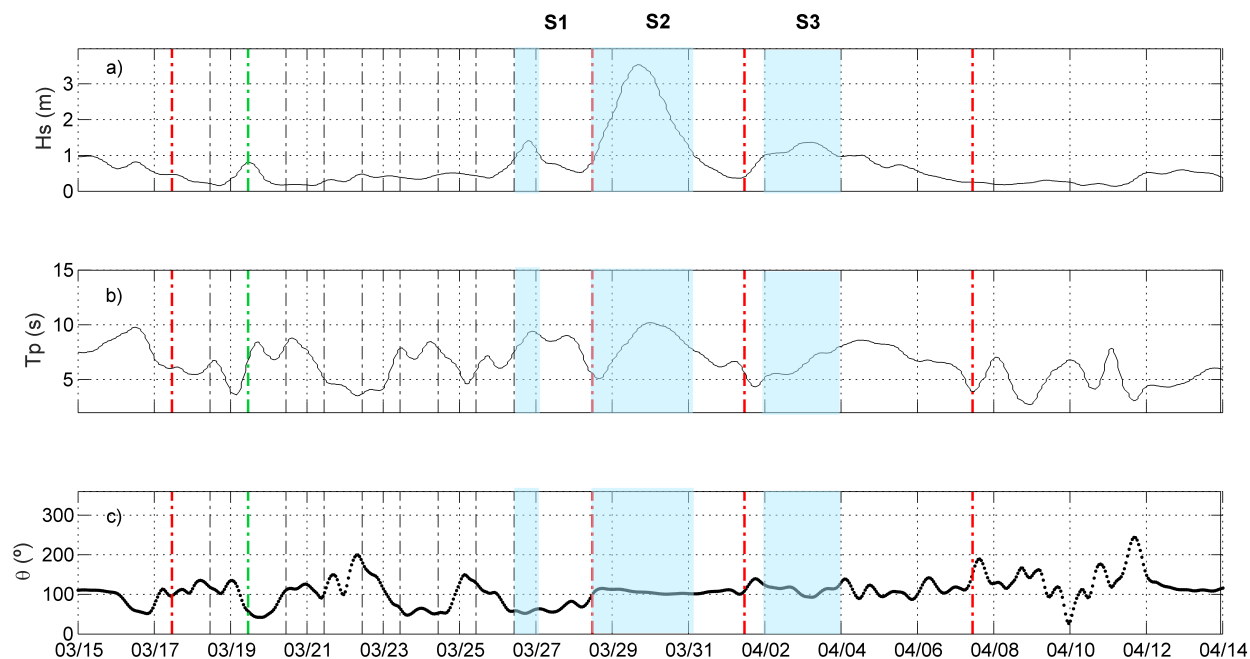
Figure 4. a) H_s (m) at $25\,\mathrm{m}$ in Cala Millor between March 15th to April 14th 2014; b) Tp (s) and c) Wave direction. The blue shading shows the period corresponding of the storms. Vertical red dotted line indicates the initial bathymetry obtained while dash dotted lines indicate the dates when cross shore profiles where measured. Vertical green dotted line states the day where the model was validated using the corresponding shore profiles. Vertical red lines show the date when bathymetry inferred from Xbeach is used for comparison betweem storms.
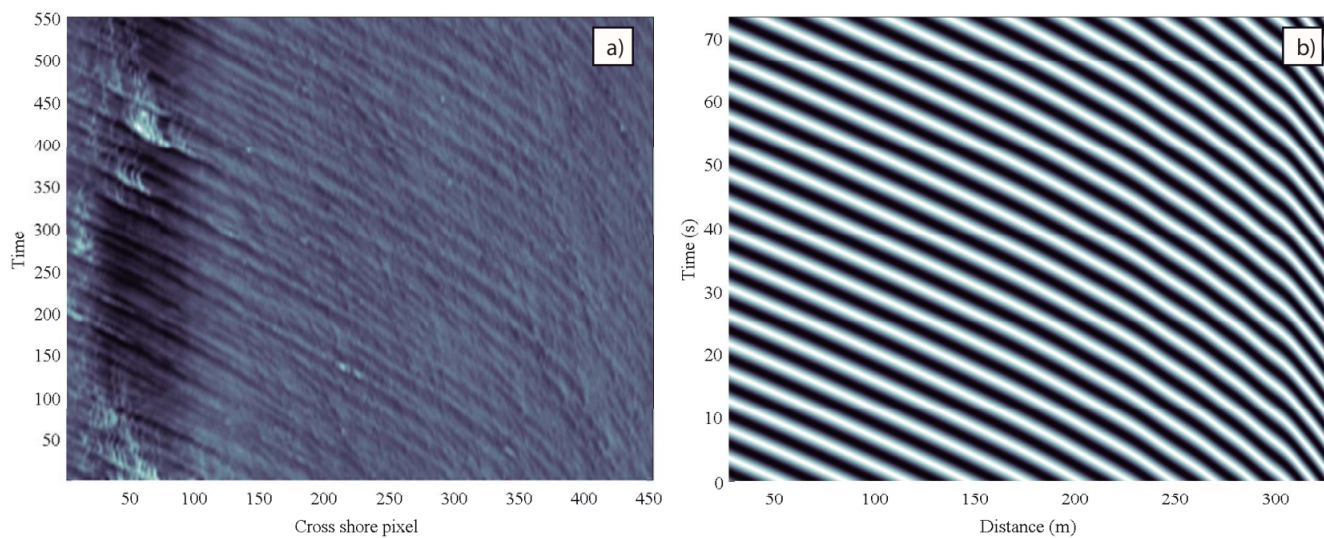
Figure 5. a) Timestack image for March 19th at 9.00 am for the central camera. The abscissa corresponds to the cross-shore direction and the ordinate for the time. b) Reconstruction for the same date assuming a constant wave height using the Fourier mode of the detected period (*i.e.* $\cos\left(\phi(x, f_w) - 2\pi\, f_w\right)$).
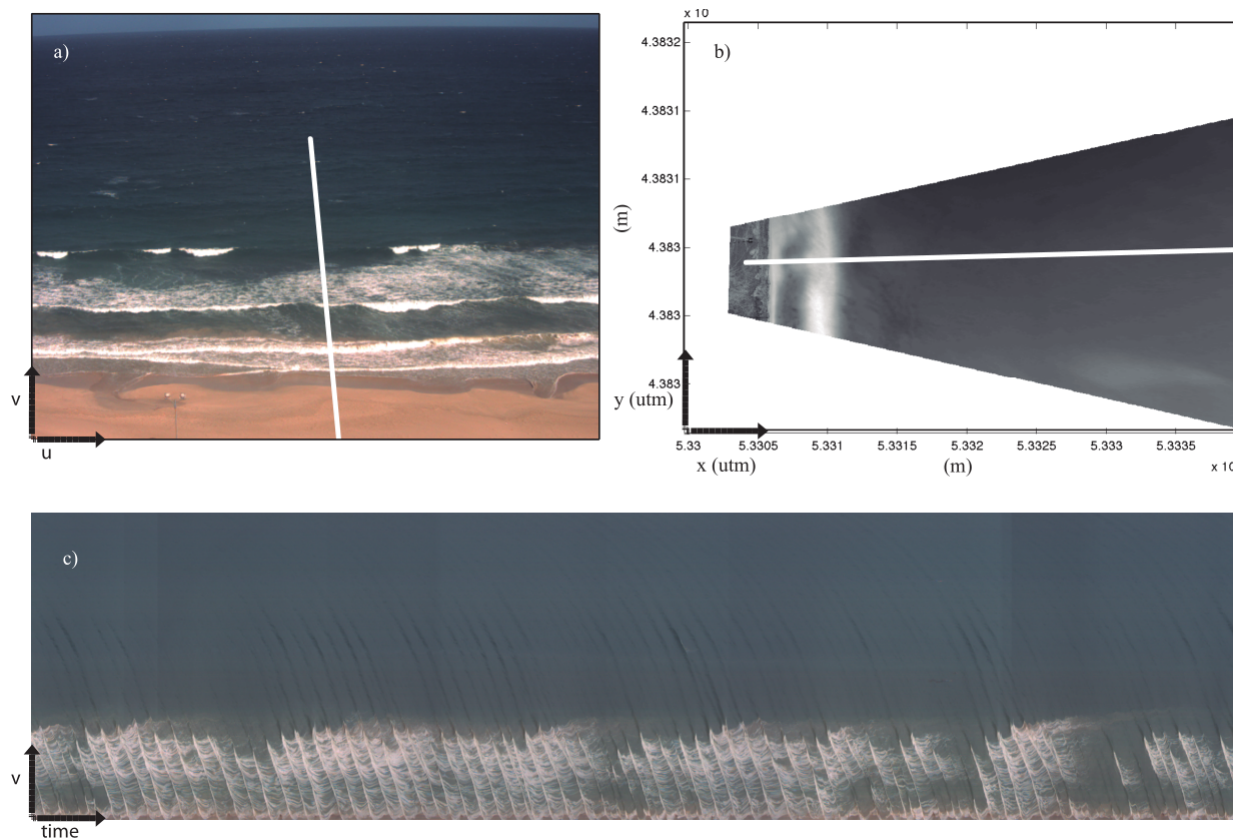
Figure 6. a) Cross-shore transect defined for the timestack image on camera #3. The Figure shows the original image in the (u, v) ≡ pixel coordinate system. b) The same after rectification in the (x, y) ≡ UTM coordinate system. c) Resulting timestack for March 19th at 10.00 am.
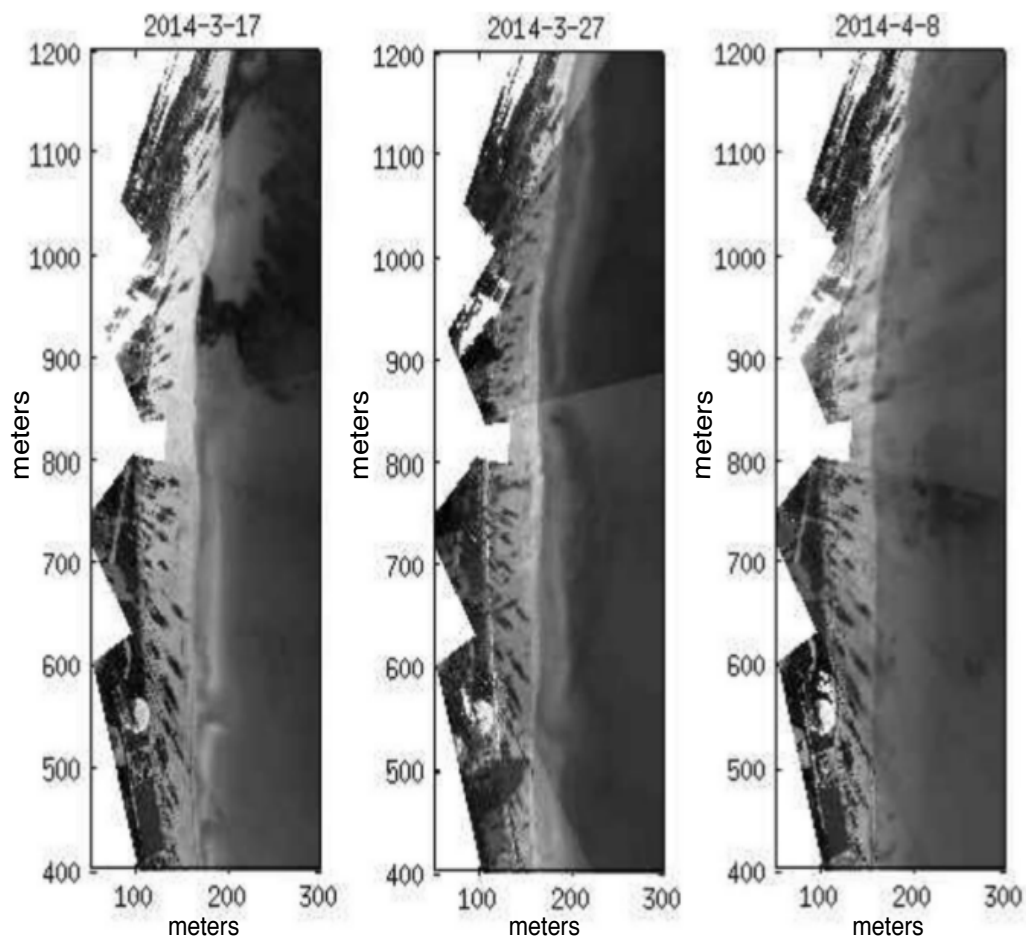
Figure 7. Timex images with dates referred in each image. Notice the intermediate configuration with a sinuous parallel bar along the coast (ca. 180 m) for March 17th and March 27th and the dissipative scenario without bar for April 8th.
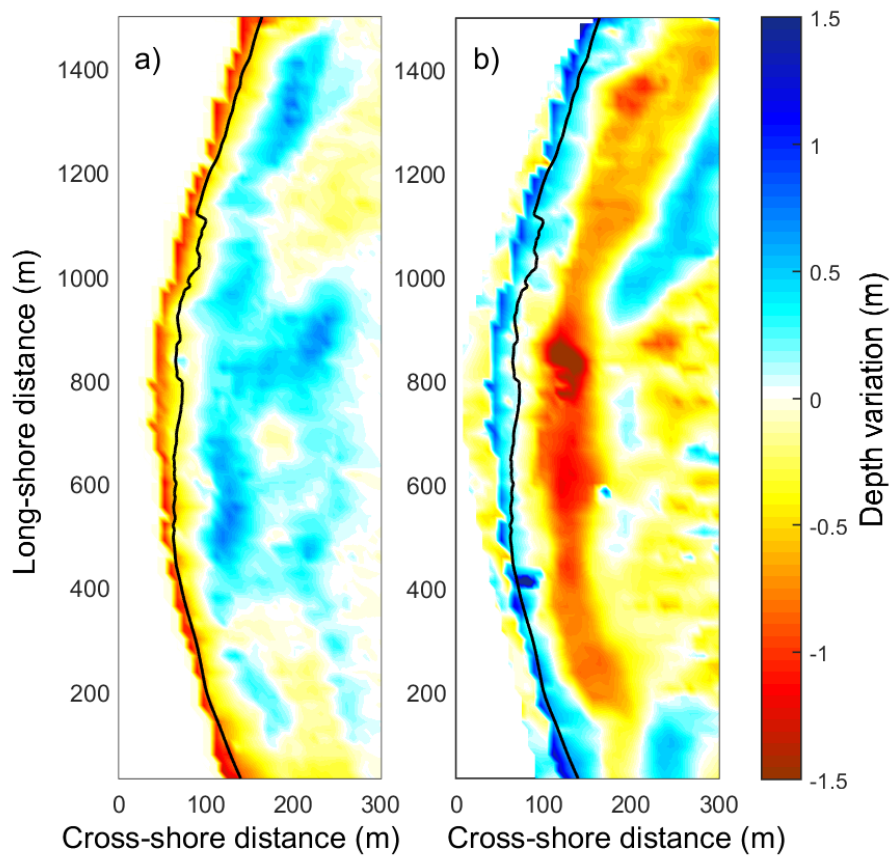
Figure 8. Depth variation estimated from XBeach and from measurements. a) Bottom variation during the storm group (March 17th to April 8th). b) Bottom variation for the period of calms (April 8th to June 12th).
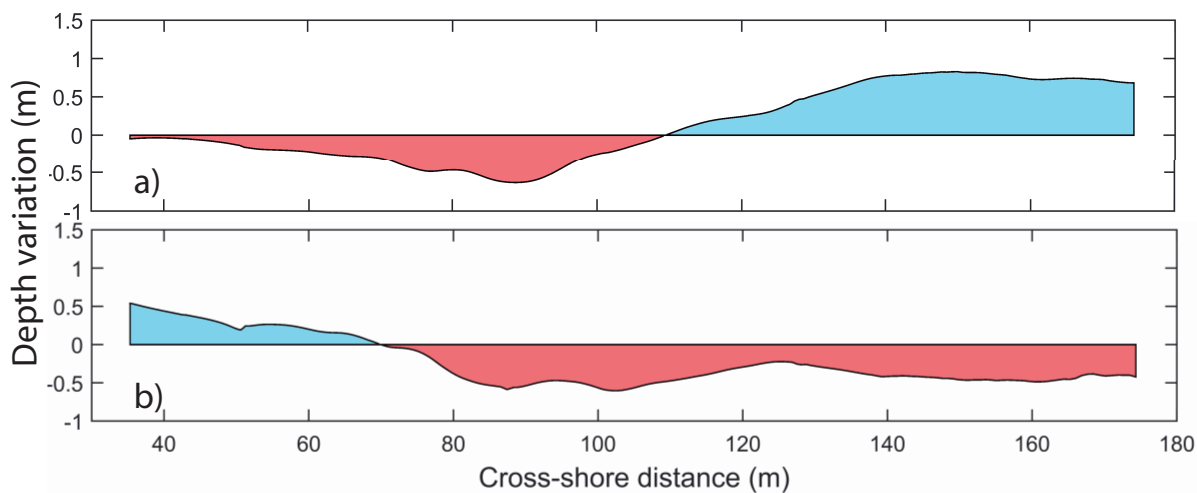
Figure 9. Depth variation estimated from bathymetry inversion of the timesatck during storm conditions; a) between April 8th and March 20th (storm conditions); b) between June 12th and April 8th (calm conditions).
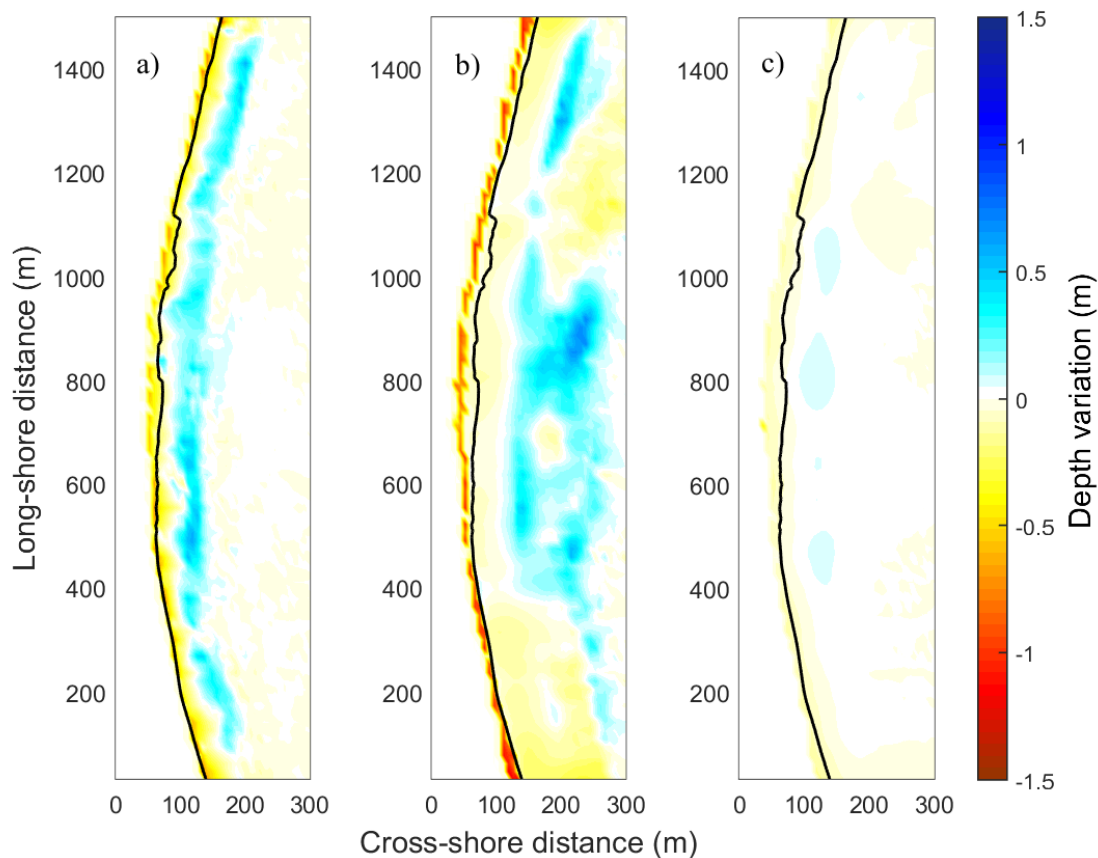
Figure 10. Depth variation estimated from XBeach and from measurements. a) Bottom variation between March 17th to March 28th (storm S1). b) Depth variation between March 28th to April 1st (storm S2). c) Depth variation between April 1st April to 8th (storm S3).